J. Acoust. Soc. Jpn. (*E*) **10**, 5 (1989)

New solutions of the wave equation for a bowed string

Takashi Kojima

Department of Computer Science, Faculty of Engineering, Shizuoka University, 3–5–1, Jouhoku, Hamamatsu, 432 Japan

(*Received 6 March 1989*)

In 1860, H. v. Helmholtz concluded, by observing the movement of each particular point of a bowed string with his vibration microscope, that the sharp bend of the bowed string travels along upper and lower parabolic arcs. Since then, his conclusion has been accepted and little attention has been paid to the shape of the envelope of the bowed string. The experimental work of M. Kondo *et al.*, which focused on this subject, stimulated the present work. This work re-examines the general solution of the wave equation by giving some initial conditions and then, in addition to the normal Helmholtz solution, obtaining two new solutions, whose shapes are of an elliptic arc and of an hyperbolic arc, respectively. These three solutions, parabolic, elliptic, and hyperbolic coincide with each other when specific parameter approaches infinity. Two experimental results found in the literature seem to represent an elliptic solution.

PACS number: 43. 40. Cw, 43. 75. De

1. INTRODUCTION

What actually happens when a string is bowed? In 1860, Hermann von Helmholtz gave clear answer to the question, observing "Lissajous figure" through his new apparatus which is called "vibration microscope." We summarize his conclusion as follows.[1] (1) The string have a sharp bend, and the string itself is stretched in two lines at any instant. (2) The bend moves backward and forward along two parabolic arcs as shown in Fig. 1. (3) The horizontal velocity of the bend is constant. This conclusion may be regarded as a good first approximation even today. Later we call this type of wave "Helmholtz motion." M. Kondo who has been studying the envelope of bowed strings experimentally, once asked me saying "Is there any possibility to get other shapes of envelope than parapolic arc by solving the differential equation mathematically?" This paper answers the question, if not fully but partly, the author hopes.

2. BASIC EQUATION AND HELMHOLTZ MOTION

Suppose the oscillation of a bowed string is the same state as free oscillation, keeping balance of energy between bowing force and dissipation in steady state. The equation of motion is written as

$$\frac{\partial^2 y}{\partial t^2}=c^2\frac{\partial^2 y}{\partial x^2} \tag{2.1}$$

where y is displacement of a string, t is time, x is distance from left end, and c is propagation velocity of transversal wave. ($c=\sqrt{T/\rho}$, T is the tension and ρ is linear density.)

The general solution of Eq. (2.1), which is called D'Alembert's solution, is shown as Eq. (2.2),

$$y(x, t)=\frac{1}{2}\{y_0(x+ct)+y_0(x-ct)\} + \frac{1}{2}\{V_0(x+ct)-V_0(x-ct)\} \tag{2.2}$$

where $y_0(x)$ is initial displacement and $V_0(x)$ is the definite integral of initial velocity $v_0(x)$.

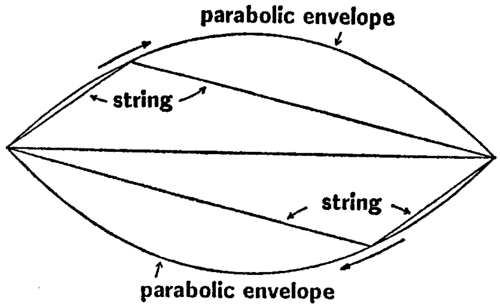

Fig. 1 "Helmholtz motion" of a bowed string. The string is stretched in the two lines, and the bend travels along upper and lower parabolic arcs. The scale of y axis is twenty times as large as that of x axis, because the amplitude of the string is very small.

$$V_0(x)=\frac{1}{c}\int_0^x v_0(\xi)d\xi \tag{2.3}$$

In the Eq. (2.2), the function with respect to $x+ct$ represents left progressive wave and the function with respect to $x-ct$ represents right progressive wave.

It is C. V. Raman who found that the following the initial conditions as the first type will make the solution exactly the same shape as that of Helmholtz motion.[2)]

$$\begin{cases} y_0(x)=0 \\ v_0(x)=v_{\max}(1-x/l) \end{cases} \tag{2.4}$$

where l is the length of a string ($0\leq x\leq l$). $v_{\max}$ is a constant, and denotes the maximum velocity.

Assume that the string is fixed at both ends, the boundary conditions are

$$y(0, t)=y(l, t)=0 \tag{2.5}$$

Setting (2.5) and $y_0(x)=0$ to Eq. (2.2), we have

$$\begin{cases} V_0(ct)=V_0(-ct) \\ V_0(l+ct)=V_0(l-ct) \end{cases} \tag{2.6}$$

Equation (2.6) means the reflection of wave on the both ends.

The substituting the velocity condition $v_0(x)$, which has the linear relation with x, into Eq. (2.3), we get

$$V_0(x)=\left(\frac{v_{\max}}{c}\right)(1-x/2l)x \tag{2.7}$$

After we examine $V_0(x)$ within the first half period of vibration ($0\leq t\leq l/c$), $V_0(x)$ during the next half period is easily calculated by using the relation

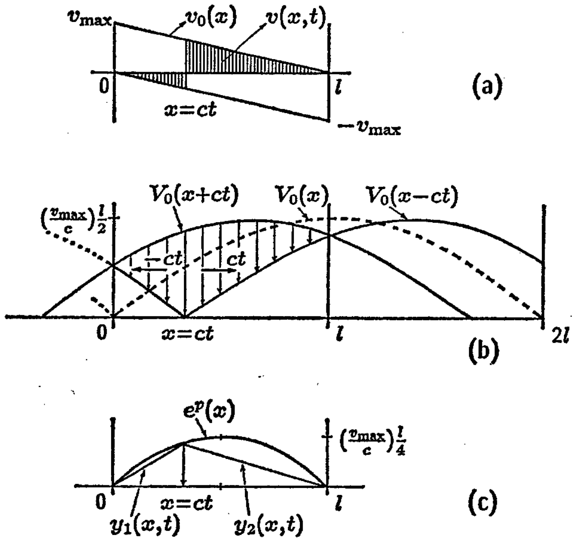

Fig. 2 Shapes of the functions $v_0(x)$, $v(x, t)$, $V_0(x)$, $y(x, t)$ and $e^p(x)$. (a) initial velocity $v_0(x)$ and velocity $v(x, t)$. (b) $V_0(x)$, $V_0(x+ct)$ and $V_0(x-ct)$. (c) displacement $y(x, t)$ and envelope $e^p(x)$.

Eq. (2.6). The envelope of $y(x, t)$ is determined by the condition that $V_0(x-ct)$ is minimum. The minimizing condition is $x=ct$. So assigning Eq. (2.2) to $x=ct$ and $y_0(x)=0$, we have envelope function

$$e(x)=\frac{1}{2}V_0(2x) \tag{2.8}$$

The substitution of $2x$ for x in Eq. (2.7) yields

$$e^p(x)=\left(\frac{v_{\max}}{c}\right)\left(1-\frac{x}{l}\right)x \tag{2.9}$$

where superscript p means "parapolic." This function represents parabolic curve. Thus the shape of an envelope is determined when we adopt the Raman's initial conditions.

Substituting $x+ct$ and $x-ct$ for x in Eq. (2.7), and putting them into Eq. (2.2) with Eq. (2.6), we have the displacement $y(x, t)$ as follows.

$$\begin{cases} y_1^p(x, t)=\left(\frac{v_{\max}}{c}\right)\left(1-\frac{ct}{l}\right)x, & (0\leq x\leq ct) \\ y_2^p(x, t)=\left(\frac{v_{\max}}{c}\right)\left(1-\frac{x}{l}\right)ct, & (ct\leq x\leq l) \end{cases} \tag{2.10}$$

Figure 2 shows the shapes of the functions $v_0(x)$, $v(x, t)$, $V_0(x)$, $e(x)$ and $y(x, t)$. It will help to understand the mutual relations between them.

We may have a question what sort of curve is possible for envelope curve if $v_0(x)$ deviate from

Raman's condition. In the next section, we will try to see how the shape changes as the initial condition changes.

3. ENVELOPE CURVE AND CONIC SECTION

When we cut off a cone by a plane with an angle to the cone axis, the cutting edge has a smooth curve. The curve is called "conic section," and it is well known that the conic section describes an arbitrary quadratic function. Let α be the angle between the cutting plane and the cone bottom plane (which is perpendicular to the cone axis). The characteristics of the function are determined by the angle. When a cutting plane is parallel to the surface line of the cone ($\alpha=\alpha^p$), the conic section becomes parabola. It becomes ellipse when $\alpha<\alpha^p$, and it becomes hyperbola when $\alpha>\alpha^p$. Figure 3 shows relation between a cutting angle α and a quadratic curve.

Now, the author re-examined the general solution of the wave equation. As a result, the envelope curve of a string is projected one to the plane which is parallel to cone axis. And it is necessary to introduce a geometric parameter r ($r>l/2$) to describe new solutions. The ratio of l to r indicates a deviation from the ideal parabolic envelope.

Let $e^p(x)$ be a parabolic envelope, and $e^e(x)$ be an elliptic one and also $e^h(x)$ be a hyperbolic one. The envelope function $e^e(x)$ is written as Eq. (3.1), and also the envelope function $e^h(x)$ is written as Eq. (3.4), where superscript e means "elliptic" and superscript h means "hyperbolic."

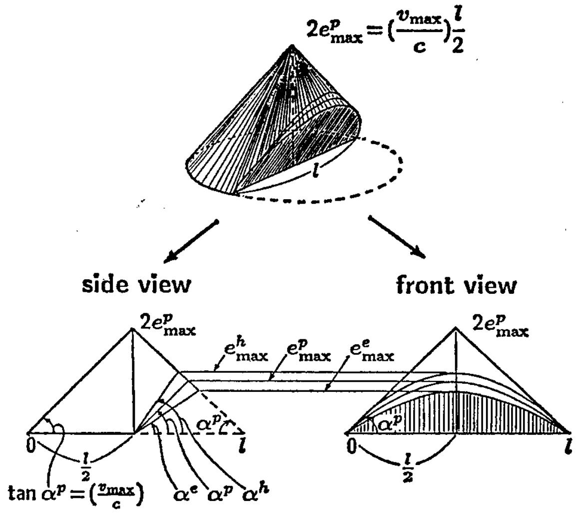

Fig. 3 Envelope curves and conic sections. Quadratic curves are classified by cutting angles.

$$e^e(x)=\left(\frac{v_{\max}}{c}\right)\frac{2d^e}{l}\left(\sqrt{r^2-(l/2-x)^2}-d^e\right) \tag{3.1}$$

where

$$d^e=\sqrt{r^2-l^2/4} \tag{3.2}$$

$$\frac{(x-x_0^e)^2}{(a^e)^2}+\frac{(e^e(x)-e_0^e)^2}{(b^e)^2}=1 \tag{3.3}$$

where

$$a^e=r\,,\quad b^e=\frac{2v_{\max}}{cl}rd^e\,,$$

$$x_0^e=l/2\,,\quad e_0^e=-\frac{2v_{\max}}{cl}(d^e)^2\,.$$

$$e^h(x)=\left(\frac{v_{\max}}{c}\right)\frac{2d^h}{l}\left(d^h-\sqrt{r^2+(l/2-x)^2}\right) \tag{3.4}$$

where

$$d^h=\sqrt{r^2+l^2/4} \tag{3.5}$$

$$\frac{(x-x_0^h)^2}{(a^h)^2}-\frac{(e^h(x)-e_0^h)^2}{(b^h)^2}=-1 \tag{3.6}$$

where

$$a^h=r\,,\quad b^h=\frac{2v_{\max}}{cl}rd^h\,,$$

$$x_0^h=l/2\,,\quad e_0^h=\frac{2v_{\max}}{cl}(d^h)^2\,.$$

$$u(x)=\left(\frac{v_{\max}}{c}\right)\frac{2d^h}{l}\left\{\pm\left(x-\frac{l}{2}\right)+d^h\right\} \tag{3.7}$$

Transposing the d^e term to left hand side in Eq. (3.1) and rewriting Eq. (3.1), we have Eq. (3.3) which represents the standard form of an ellipse. And also rewriting Eq. (3.4), we have Eq. (3.6) which represents the standard form of a hyperbola. Equation (3.7) represents two asymptotic lines of Eq. (3.6). Three envelope curves, the asymptotic lines of Eq. (3.6) and the location of the center of Eq. (3.3) are shown in Fig. 4 to help understanding the geometric relations.

Let's consider the highest point of an envelope curve. An envelope curve has the maximum at the point $x=l/2$. $e^e_{\max}$, $e^p_{\max}$ and $e^h_{\max}$ denote the maxima of envelope are given by Eq. (3.8), Eq. (3.9) and Eq. (3.10) respectively.

$$e^e_{\max}=e^e\left(\frac{l}{2}\right)=\left(\frac{v_{\max}}{c}\right)\frac{l}{2}\frac{d^e}{r+d^e} \tag{3.8}$$

$$e^p_{\max}=e^p\left(\frac{l}{2}\right)=\left(\frac{v_{\max}}{c}\right)\frac{l}{4} \tag{3.9}$$

$$e^h_{\max}=e^h\left(\frac{l}{2}\right)=\left(\frac{v_{\max}}{c}\right)\frac{l}{2}\frac{d^h}{r+d^h} \tag{3.10}$$

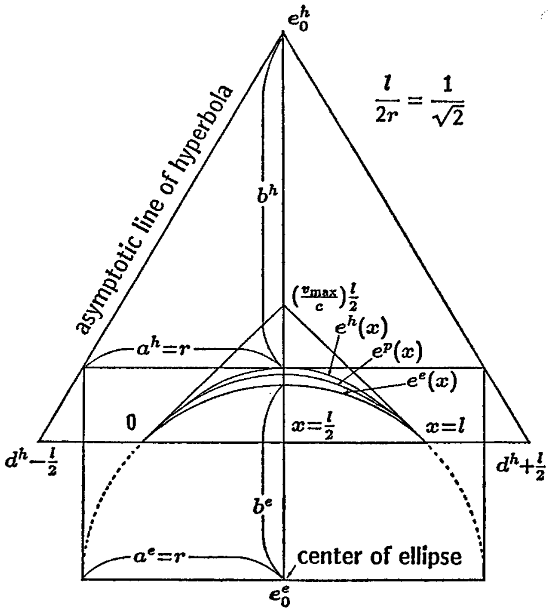

Fig. 4 Geometric relation among three envelope curves. It is shown the asymptotic lines of a hyperbola and the center of an ellipse, in addition to three envelope curves.

$$e_{max}^e \leq e_{max}^p \leq e_{max}^h \tag{3.11}$$

If $r \gg l/2$ then $d^e/(r+d^e) \to 1/2$ and $d^h/(r+d^h) \to 1/2$, so we have the relation (3.11). Three curves are indistinguishable from each other when $r \gg l/2$ or $2r/l \to \infty$.

The gradient of a tangential line at left end $(x=0)$ is calculated from the first derivative of $e(x)$. Calculating in three cases, the results are written as Eq. (3.12). The gradients are equal to each other. Similarly the gradients at right end $(x=l)$ in three cases are written as Eq. (3.13).

$$\left.\frac{de^e}{dx}\right|_{x=0}=\left.\frac{de^p}{dx}\right|_{x=0}=\left.\frac{de^h}{dx}\right|_{x=0}=\left(\frac{v_{max}}{c}\right) \tag{3.12}$$

$$\left.\frac{de^e}{dx}\right|_{x=l}=\left.\frac{de^p}{dx}\right|_{x=l}=\left.\frac{de^h}{dx}\right|_{x=l}=-\left(\frac{v_{max}}{c}\right) \tag{3.13}$$

The angles between three cutting planes and the bottom plane of the cone in Fig. 3 are calculated as follows.

$$\alpha^e=\arctan\left(\frac{v_{max}}{c}\sqrt{1-\left(\frac{l}{2r}\right)^2}\right) \tag{3.14}$$

$$\alpha^p=\arctan\left(\frac{v_{max}}{c}\right) \tag{3.15}$$

$$\alpha^h=\arctan\left(\frac{v_{max}}{c}\sqrt{1+\left(\frac{l}{2r}\right)^2}\right) \tag{3.16}$$

$$\alpha^e \leq \alpha^p \leq \alpha^h \tag{3.17}$$

It is obvious that we get the relation (3.17).

4. SHAPE OF STRING AND APEX ANGLE

When the envelope function $e(x)$ is given, we can obtain the initial velocity $v_0(x)$ for the new types by solving Eq. (2.8) and Eq. (2.3). The initial velocity functions for the new types are calculated as follows.

$$v_0^e(x)=v_{max}\frac{d^e}{\sqrt{r^2-(l-x)^2/4}}(1-x/l) \tag{4.1}$$

$$v_0^h(x)=v_{max}\frac{d^h}{\sqrt{r^2+(l-x)^2/4}}(1-x/l) \tag{4.2}$$

These functions Eq. (2.4), Eq. (4.1) and Eq. (4.2) are shown in Fig. 5. Also $y_1(x, t)$ and $y_2(x, t)$ are calculated as follows.

$$\begin{cases} y_1^e(x)=\left(\frac{v_{max}}{c}\right)\frac{2d^e}{l}\{\sqrt{r^2-(l-x-ct)^2/4} \\ \qquad -\sqrt{r^2-(l+x-ct)^2/4}\}, \\ \qquad (0\leq x\leq ct) \\ y_2^e(x)=\left(\frac{v_{max}}{c}\right)\frac{2d^e}{l}\{\sqrt{r^2-(l-x-ct)^2/4} \\ \qquad -\sqrt{r^2-(l-x+ct)^2/4}\}, \\ \qquad (ct\leq x\leq l) \end{cases} \tag{4.3}$$

$$\begin{cases} y_1^h(x)=\left(\frac{v_{max}}{c}\right)\frac{2d^h}{l}\{\sqrt{r^2+(l+x-ct)^2/4} \\ \qquad -\sqrt{r^2+(l-x-ct)^2/4}\}, \\ \qquad (0\leq x\leq ct) \\ y_2^h(x)=\left(\frac{v_{max}}{c}\right)\frac{2d^h}{l}\{\sqrt{r^2+(l-x+ct)^2/4} \\ \qquad -\sqrt{r^2+(l-x-ct)^2/4}\}, \\ \qquad (ct\leq x\leq l) \end{cases} \tag{4.4}$$

It is difficult to see without magnifying of y axis, because the amplitude of a string is very small. If

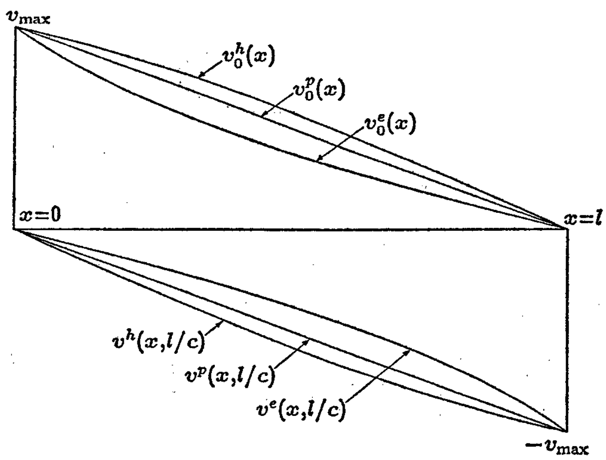

Fig. 5 Shapes of initial velocity $v_0(x)$ and that of velocity $v(x, l/c)$ in three cases.

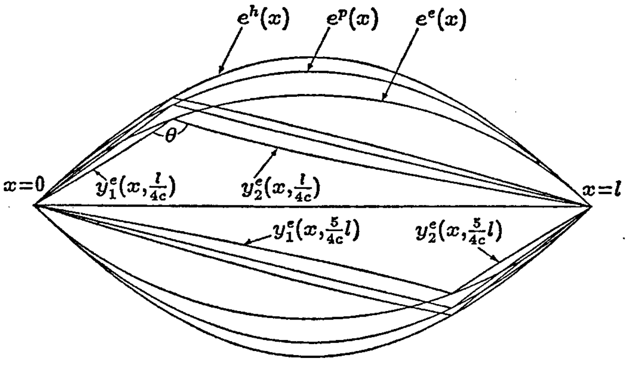

Fig. 6 Shapes of string at $t=l/4c$ and $t=5l/4c$ in three cases. The string curves inward on upper and lower side in the case of an elliptic envelope, and curves outward on upper and lower side in the case of a hyperbolic envelope.

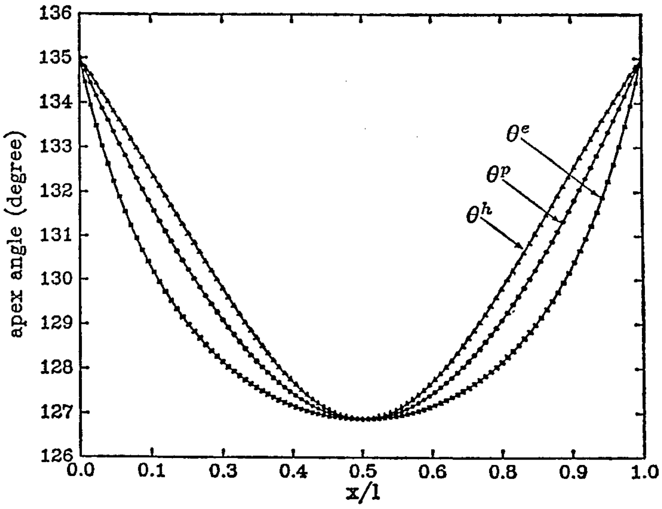

Fig. 7 Changes of apex angle with x. In this case, the amplitude of the string is magnified $(c/v_{\max})$ times.

we magnify y axis $(c/v_{\max})$ times, then the maximum of the envelope in a parabolic case is $l/4$. For example, when $l=320$ mm and $e^p_{\max}=4$ mm, the magnifying power $(c/v_{\max})$ is twenty, which is calculated from Eq. (3.9). With the magnifying of y axis, the envelope curves and the shapes of a string (at $t=l/4c$ and at $t=5l/4c$) are shown in Fig. 6. The geometric parameter r is selected $2r/l=\sqrt{2}$ in this case.

Now, we discuss the angle between $y_1(x, t)$ and $y_2(x, t)$. The angle, which is called apex angle, is defined by Eq. (4.5). The apex angles in three cases are written as Eq. (4.6), Eq. (4.7) and Eq. (4.8).

$$\theta=\pi-\left\{\arctan\left(\left.\frac{\partial y_1}{\partial x}\right|_{x=ct}\right)+\arctan\left(-\left.\frac{\partial y_2}{\partial x}\right|_{x=ct}\right)\right\} \tag{4.5}$$

$$\theta^p=\pi-\left\{\arctan\left(\left(\frac{v_{\max}}{c}\right)\left(1-\frac{ct}{l}\right)\right)+\arctan\left(\left(\frac{v_{\max}}{c}\right)\left(\frac{ct}{l}\right)\right)\right\} \tag{4.6}$$

$$\theta^e=\pi-\left\{\arctan\left[\left(\frac{v_{\max}}{c}\right)\left\{\frac{1}{2}+\frac{d^e}{\sqrt{r^2-(l-2ct)^2/4}}\left(\frac{1}{2}-\frac{ct}{l}\right)\right\}\right]+\arctan\left[\left(\frac{v_{\max}}{c}\right)\left\{\frac{1}{2}-\frac{d^e}{\sqrt{r^2-(l-2ct)^2/4}}\left(\frac{1}{2}-\frac{ct}{l}\right)\right\}\right]\right\} \tag{4.7}$$

$$\theta^h=\pi-\left\{\arctan\left[\left(\frac{v_{\max}}{c}\right)\left\{\frac{1}{2}+\frac{d^h}{\sqrt{r^2+(l-2ct)^2/4}}\left(\frac{1}{2}-\frac{ct}{l}\right)\right\}\right]+\arctan\left[\left(\frac{v_{\max}}{c}\right)\left\{\frac{1}{2}-\frac{d^h}{\sqrt{r^2+(l-2ct)^2/4}}\left(\frac{1}{2}-\frac{ct}{l}\right)\right\}\right]\right\} \tag{4.8}$$

Figure 7 shows the changes of three apex angles with x magnifying y axis as same as Fig. 6. As a result, apex angles are not constant, smaller at the center than at both ends in all cases.

5. THEORETICAL WAVE FORM AND OBSERVED WAVE FORM

The displacement wave form along time axis is calculated from $y(x, t)$. We select the point $x=l/4$. Figure 8 shows the displacement wave forms in three cases within one period. That is ideal saw tooth wave

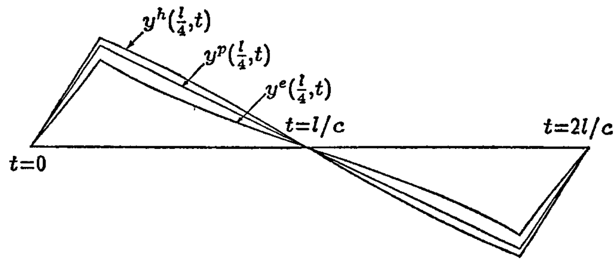

Fig. 8 Displacement wave forms within one period at $x=l/4$.

in the case of a parabolic envelope. Within the first half period, the curve of displacement in the case of an elliptic envelope have positive curvature (, or the center of curvature is located above the curve). That in the case of a hyperbolic envelope have negative curvature (, or the center of curvature is located below the curve).

The velocity function $v(x, t)$ is calculated as the first partial derivative of $y(x, t)$ with respect to t.

$$\begin{cases} v_1(x, t)=\dfrac{\partial y_1}{\partial t}, & (0\leq x\leq ct) \\ v_2(x, t)=\dfrac{\partial y_2}{\partial t}, & (ct\leq x\leq l) \end{cases} \tag{5.1}$$

The substitution of Eq. (2.10) into Eq. (5.1) yields Eq. (5.2). And also the substitution of Eq. (4.3) into Eq. (5.1) yields Eq. (5.3). Equation (5.4) is obtained by using Eq. (4.4) as same as Eq. (5.3).

$$\begin{cases} v_1^p(x, t)=-v_{\max}\dfrac{x}{l}, & (0\leq x\leq ct) \\ v_2^p(x, t)=v_{\max}\left(1-\dfrac{x}{l}\right), & (ct\leq x\leq l) \end{cases} \tag{5.2}$$

$$\begin{cases} v_1^e(x, t)=\dfrac{v_{\max}}{2}\dfrac{d^e}{l}\left\{\dfrac{+(l-x-ct)}{\sqrt{r^2-(l-x-ct)^2/4}}-\dfrac{-(l+x-ct)}{\sqrt{r^2-(l+x-ct)^2/4}}\right\}, \\ \qquad (0\leq x\leq ct) \\ v_2^e(x, t)=\dfrac{v_{\max}}{2}\dfrac{d^e}{l}\left\{\dfrac{+(l-x-ct)}{\sqrt{r^2-(l-x-ct)^2/4}}-\dfrac{+(l-x+ct)}{\sqrt{r^2-(l-x+ct)^2/4}}\right\}, \\ \qquad (ct\leq x\leq l) \end{cases} \tag{5.3}$$

$$\begin{cases} v_1^h(x, t)=\dfrac{v_{\max}}{2}\dfrac{d^h}{l}\left\{\dfrac{-(l+x-ct)}{\sqrt{r^2+(l+x-ct)^2/4}}-\dfrac{-(l-x-ct)}{\sqrt{r^2+(l-x-ct)^2/4}}\right\}, \\ \qquad (0\leq x\leq ct) \\ v_2^h(x, t)=\dfrac{v_{\max}}{2}\dfrac{d^h}{l}\left\{\dfrac{+(l-x+ct)}{\sqrt{r^2+(l-x+ct)^2/4}}-\dfrac{-(l-x-ct)}{\sqrt{r^2+(l-x-ct)^2/4}}\right\}, \\ \qquad (ct\leq x\leq l) \end{cases} \tag{5.4}$$

The velocity wave forms are calculated from (5.2), (5.3) and (5.4) as shown in Fig. 9. That is ideal rectangular wave in the case of the parabolic envelope. The shape of an elliptic case is like a concave lens, curves inward on upper and lower side. And the shape of a hyperbolic case is like a convex lens, curves outward on upper and lower side.

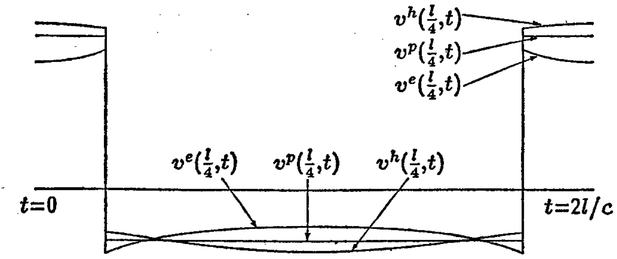

Fig. 9 Velocity wave forms within one period at $x=l/4$.

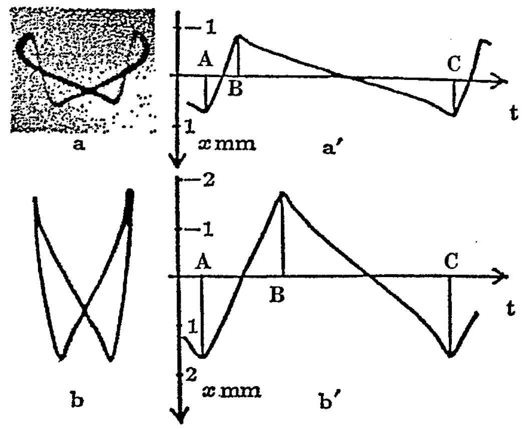

a: observed point; x = 4.0 cm on G bow; z = 3.3 cm, $+x$, 34.2 cm/sec
b: observed point; x = 10.0 cm on G bow; z = 3.3 cm, $+x$, 34.2 cm/sec

Fig. 10 Observed displacement wave forms by A. Kuni and M. Kondo.[3] The form in each case curves slightly like an elliptic envelope as shown in Fig. 8.

For comparison between theoretical wave form and observed wave form, the author reviewed much literature. As a result, two examples corresponding to elliptic case are found as shown in Fig. 10[3] and in Fig. 11,[4] but no example is found corresponding to a hyperbolic case until now.

6. CONCLUSION

The wave equation of a string have three solutions, whose envelopes are of an elliptic arc, of a parabolic arc and of a hyperbolic arc. These three solutions are

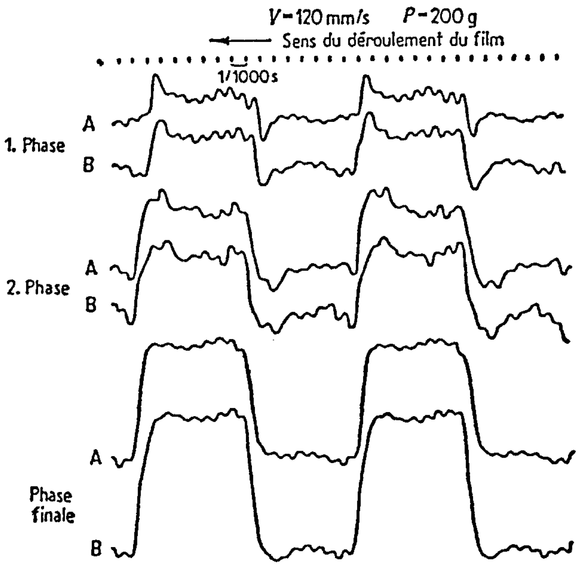

Graphiques de la vitesse de vibration, obtenue à $l/2$, pendant l'état transitoire, puis stationnaire (phase finale), avec duex méthodes: A) électromagnétique; B) électrostatique, qui mettent en évidence une forme d'onde sensiblement la même. Humidité = 65%, V = 120 mm/s, P = 200 g.

Fig. 11 Observed velocity wave forms by B. Bladier.[4] The form in each case is concave like an elliptic envelope as shown in Fig. 9.

indistinguishable from each other when a specific parameter approaches infinity. Two experimental results found in the literature seem to represent an elliptic solution.

ACKNOWLEDGMENT

The author would like to thank Emeritus Prof. Masao Kondo of Gakushuin University and Prof. Isao Nakamura of University of Electrocommunications for their helpful advice and encouragement.

REFERENCES

1) H. Helmholtz, *On the Sensations of Tone* (Dover Publications Inc., New York, 1954), p. 387
2) C. V. Raman, "On the mechanical theory of the vibrations of bowed strings and of musical instruments of the violin family, with experimental verification of the results: Part I," Indian Assoc. Cultiv. Sci. Bull. **15**, 1–31 (1918).
3) A. Kuni and M. Kondo, "An experimental study on a bowed string," 6th Int. Congr. Acoust., N-2-4, Tokyo (1968).
4) B. Bladier, "Contribution a l'etude des codes du violoncelle," Acustica **11**, 373–384 (1961).